Article

Investigation of the Dielectric Properties of Graphite and Carbon Black-Filled Composites as Electromagnetic Interference Shielding Coatings

Emre Gümüş [1,2,*] , Mustafa Yağımlı [3] and Emin Arca [4]

1 Gedik Vocational School, Istanbul Gedik University, 34913 Istanbul, Turkey
2 Occupational Safety Department, Institute of Pure and Applied Sciences, Marmara University, 34722 Istanbul, Turkey
3 Faculty of Engineering, Istanbul Gedik University, 34876 Istanbul, Turkey; mustafa.yagimli@gedik.edu.tr
4 Faculty of Engineering, Marmara University, 34722 Istanbul, Turkey; earca@marmara.edu.tr
* Correspondence: emre.gumus@gedik.edu.tr

Abstract: The main purpose of electromagnetic interference (EMI) shielding coatings is the insulation of sensitive devices and protect people from electromagnetic field exposure due to its effects on the human body. This paper investigates the dielectric properties, and electromagnetic shielding performances of graphite and carbon black (CB) filled epoxy matrix composites produced by the mechanical mixing method. The sample compositions were created at rates ranging from 1 to 7 wt%. Samples were analyzed by Vector Network Analyzer (VNA) using the coaxial method in the range of 1–14 GHz, including L band, S band, C band, X band and partially Ku band. After determining the scattering parameters with VNA, AC conductivity, absorption, reflection and total shielding efficiency values were calculated. At high frequencies, almost all the samples showed higher AC conductivity. CB-filled samples show higher AC conductivity than graphite-filled samples. The total shielding efficiency (SE_T) of the graphite-added samples (19–21 dB) is slightly higher than the carbon black-added samples (8–17 dB). Distinct filling ratios in graphite-added samples result in closer shielding behavior in contrast to carbon black-added samples. However, higher shielding efficiency is observed as the CB filler ratio increases. The shielding efficiencies of the samples with both types of filling materials vary little depending on the frequency. Reflection is the main mechanism of the shielding efficiency, which constitutes the majority of total efficiency for all types of samples.

Keywords: coating; electromagnetic interference shielding; composites; carbon black; graphite

1. Introduction

Electromagnetic interference (EMI) shielding has become an increasingly important area of research due to the increase of electronic device usage in our daily lives. With the rising demand for electronic and telecommunication devices [1], as well as the increasing concern over EMI on human health and safety, the need for effective shielding materials has become paramount [2]. Recent studies have determined the effects of electromagnetic waves on the human body [3–6]. These negative effects can be avoided by isolating places where people use sensitive electronic devices are located. For example, International Commission on Non-Ionizing Radiation Protection (ICNIRP) provides guidelines and recommendations for limiting human exposure to electromagnetic fields in the frequency range of 0 Hz to 300 GHz. Their guidelines cover both occupational and public exposure and are based on scientific research and expert consensus. International Electrotechnical Commission (IEC) publishes standards related to the safety and effectiveness of electrical and electronic devices, including limits on human exposure to electromagnetic radiation. Institute of Electrical and Electronics Engineers (IEEE) has developed standards, such as

IEEE C95.1, which provides guidelines for safety levels with respect to human exposure to electric, magnetic and electromagnetic fields.

The 1–14 GHz frequency range is commonly referred to as the microwave frequency range. It includes a range of electromagnetic waves with relatively high frequencies and shorter wavelengths compared to radio waves and lower-frequency signals. This range includes L-band (1–2 GHz), S-band (2–4 GHz), C-band (4–8 GHz), X-band (8–12 GHz) and partial Ku-band (12–18 GHz). These bands are used for telecommunications (communication systems, microwave links, satellite communication, radar systems etc.), wireless networks (Wi-Fi, Bluetooth, microwave-based wireless local area networks etc.), aerospace and defense (aircraft navigation, weather monitoring, target detection, surveillance etc.), medical imaging, scientific research (spectroscopy, radio astronomy etc.), industrial applications (microwave heating, drying, sterilization etc.) and automotive radar (collision avoidance systems, adaptive cruise control etc.) [7].

When an electromagnetic wave penetrates a material, the wave can be transmitted, absorbed, or reflected, depending on the properties of the material and the characteristics of the wave. Transmission occurs when the wave passes through the material without being attenuated. This can occur if the material has a low impedance and is of the same order of magnitude as the wave impedance [8]. Absorption occurs when the energy of the wave is dissipated within the material. This is typically due to the resistive losses of the material, which convert the electromagnetic energy into heat. The amount of absorption depends on the conductivity of the material and the frequency of the wave [9,10]. Reflection occurs when the wave is reflected into the medium from which it originated. This can occur if the shielding material has a high impedance and is not of the same order of magnitude as the wave impedance. The reflection coefficient, which is a measure of the amount of energy reflected, depends on the difference in impedance between the material and the medium [11].

EMI shielding can be provided by using metallic products, such as copper, silver, iron, nickel, etc., that have reflectiveness due to high electrical conductivity [12,13]. When metals are used for these applications, some characteristics such as high density, poor corrosion resistance and forming difficulty must be dealt with [14]. Among the various materials being investigated for electromagnetic shielding, carbon-based materials, such as graphite, carbon black, carbon fiber, carbon nanotube and graphene, have shown great promise due to their high electrical conductivity, low density, easy processing and low cost [15,16]. These materials can effectively absorb and dissipate electromagnetic radiation, making them ideal candidates for use in electromagnetic shielding applications. Herewith, a composite material in a polymer matrix with high shielding efficiency can be produced [17]. Several polymers are used for polymer matrices, such as polyaniline, polyurethane, ethylene methyl acrylate, epoxy, and polypropylene. Apart from these types of materials, different alternative materials like multilayer nanocomposites [18,19], wood-based composites [20,21], metalized carbon fabric [22] and carbonyl iron powder dispersed thermoplastic polyurethane composites with metal mesh layer [23] are also being investigated by other researchers. Whether the electromagnetic shielding is good or bad does not the only thing determining the type of material to be selected. For the structure, vehicle, or device to be shielded, its mechanical properties, conditions of use and cost are other factors to consider.

The dielectric properties of a polymer composite are affected by the permittivity, conductivity, and weight percentage of the filler added to the composite material. The effective electromagnetic shielding of polymer composites greatly depends on the distribution of individual carbon-based fillers within the polymer matrix. The electron percolation between the separated particles affects the electrical conductivity of the composites. In order to achieve effective electromagnetic shielding, high content and good dispersion of carbon-based materials are usually necessary. The addition of a significant amount of conductive carbon-based fillers can have negative effects on the mechanical properties and processibility of the composites. This is due to severe agglomeration and poor filler–matrix bonding,

which can result in worse conductivity and bad surface morphology [24]. Therefore, the production method plays an important role as much as the material in electromagnetic shielding [25]. There are several production methods used for EMI shielding polymer composites. The selection of a particular method depends on factors such as the desired composite properties, the type of polymer matrix, the type and distribution of the filler material, available manufacturing capabilities and the required production scale. Examples of these methods are solution mixing, melt mixing, mechanical mixing, electrospinning, and in-situ polymerization.

Graphite provides electromagnetic shielding due to its conductive properties. It is a well-known allotrope of carbon, and its 2D structure is composed of layers of carbon atoms arranged in a hexagonal lattice. Each carbon atom forms three covalent bonds with adjacent carbon atoms, creating a flat, honeycomb-like structure. The 2D structure of graphite allows it to conduct electricity along its layers, making it an effective conductor of electric current. In the manufacturing of polymer composites, the addition of graphite acts as a beneficial enhancement, enhancing both mechanical and electrical properties. Polymer matrix graphite-filled composites exhibit high electromagnetic shielding efficiency at high frequencies due to the conductive nature of graphite. The high conductivity of graphite enables it to create numerous conductive pathways within the composite material, thereby facilitating the absorption and reflection of electromagnetic radiation [26]. Additionally, the presence of epoxy in the composite material enhances its mechanical and thermal stability, which makes it a suitable candidate for a wide range of applications in various industries [27,28].

Carbon black is a form of finely divided carbon that is primarily composed of elemental carbon. It is produced through the incomplete combustion or thermal decomposition of hydrocarbons, such as natural gas or petroleum products. Carbon black particles are typically small and have a high surface area, which gives them unique properties like reinforcement, conductivity, and pigmentation. As the carbon black content increases in a composite material, the electromagnetic shielding efficiency generally increases. This is because carbon black is a conductive material that can absorb and dissipate electromagnetic radiation [29]. The increase in carbon black content provides more conductive pathways for the electromagnetic waves to be absorbed and dissipated, thus increasing the shielding efficiency [30]. However, the relationship between carbon black content and electromagnetic shielding efficiency may not always be linear. At higher carbon black loadings, the shielding efficiency may begin to level off or even decrease due to factors such as agglomeration, loss of dispersibility, or changes in the material's physical properties. The optimal carbon black loading for achieving maximum electromagnetic shielding efficiency depends on various factors, such as the type of carbon black, the composite matrix, and the operating frequency range [31].

In this study, the dielectric properties of epoxy matrix composites containing graphite and carbon black were investigated, and their EMI shielding performances were determined at low filler ratios. Different graphite and carbon black additive ratios with epoxy matrix combinations have been tried and compared with each other. This type of composite can be molded and produced in plate form. It can be applied as a low-cost solution with a suitable adhesive to the walls of a fixed structure where shielding is needed.

2. Materials and Methods

2.1. Materials

Table 1 presents the compositions of the epoxy matrix samples, indicating the weight percentages of CB and graphite used in the study. The range of filler concentrations varied from 1 to 7 wt%, allowing for the investigation of their effects on the electromagnetic shielding performance of the composite materials. Both CB and graphite are in powder form, while the epoxy resin is in liquid resin form. CB's average particle size is 10 μm, and graphite's average particle size is 30 μm.

Table 1. Graphite and carbon black-filled sample compositions.

Graphite Filled	Carbon Black Filled	Matrix	Fillet Ratio in Weight %
G1	CB1		1
G3	CB3	Epoxy	3
G5	CB5		5
G7	CB7		7

Epoxy is typically composed of two main components: a resin and a hardener. The resin is a viscous liquid, and the hardener is a curing agent. When these two components are mixed, a chemical reaction occurs, resulting in the curing of the epoxy. The resin and hardener react to form cross-linked polymer chains, creating a strong and durable solid material. It typically exhibits low shrinkage during curing, ensuring dimensional stability.

Cycloaliphatic amine is used as a curing agent for the epoxy. The resin-to-curing agent ratio is 2:1.

2.2. Sample Preparation

For sample preparation mechanical mixing method is used because it's simple and doesn't require expensive equipment. The process of producing polymer composites typically involves mixing polymer powder or resin with filler, using mechanical mixing equipment like a kneader. However, if the filler powder has a fine particle size or a higher density than the polymer matrix, the powder particles may segregate. This situation makes it difficult to uniformly disperse filler particles in the polymer matrix and ultimately leading to a difference in the final product's performance [32]. Since carbon black has fine particle size, sample integrity could not be achieved in compositions above 7 wt% in the mechanical mixing production method.

Curing agent cycloaliphatic amine was added to the epoxy resin and stirred first. Then powder components were added and mechanically mixed for 15 min. The mixture was poured into the mold at 2 mm thickness and left to cure at room temperature to form crosslinks in the matrix. So, 50 × 60 mm plate-shaped specimens were formed.

Since the samples were of regular shape, size measurements were made with a micrometer. After weighting, sample densities were calculated according to mass/volume, as shown in Table 2.

Table 2. Sample densities.

Graphite Filled	Density g/cm^3	Carbon Black Filled	Density g/cm^3
G1	1.310	CB1	1.306
G3	1.341	CB3	1.318
G5	1.348	CB5	1.330
G7	1.373	CB7	1.342

In order to perform the measurement procedure with the coaxial method at the vector network analyzer, a doughnut shape plate possessing an outer diameter of 7 mm is preferred. We cut out a piece having a 3 mm diameter from the center of the plate, as shown in Figure 1. Sample surfaces were sanded with emery paper to be smooth. The sample thickness remained at 2 mm so that the samples' sizes and shapes were adapted to the coaxial probe.

2.3. Vector Network Analyzer

A Vector Network Analyzer (VNA) is a precision electronic instrument used to measure the electrical properties of microwave devices, components, and systems. The primary

function of a VNA is to analyze the transmission and reflection characteristics of electrical networks. It measures and displays the complex-valued scattering parameters.
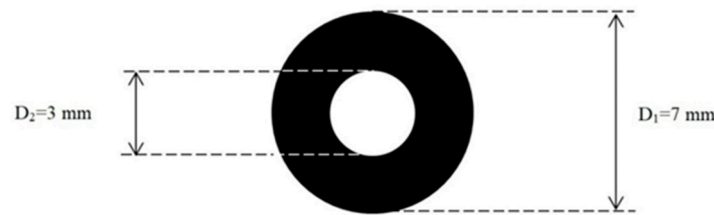

Figure 1. Specimen dimensions for co-axial method.

The coaxial method was used to determine the shielding efficiency. One significant benefit of this technique is its comparability across different laboratories, as the results obtained can be easily compared. Moreover, using a coaxial transmission line allows for the resolution of the data into its reflected, absorbed, and transmitted components. The measurements can be performed at specific frequencies by utilizing a modulated signal generator, crystal detector, and tuned amplifier.

The measurements are carried out by measuring the scattering parameters S11, S12, S21, and S22 (Figure 2) between 1–14 GHz according to the coaxial method, then dielectric parameters, including both real (ε') and imaginary parts (ε'') were derived using the Keysight N1500 software. Measurements were taken every 65 MHz at room temperature.
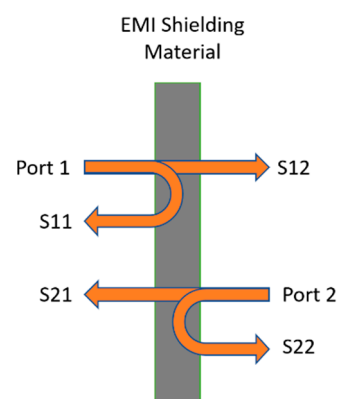

Figure 2. Scattering parameters.

Nicolson–Ross–Weir method, which is widely used in the derivation of dielectric parameters, the polynomial model in the software is carried out since it produces suitable results for materials without magnetic components, which eliminates discontinuity points that occur due to sample thickness [33]. Its algorithm is a computer-based technique that is utilized to indirectly obtain the dielectric properties of a material [34]. It achieves this by analyzing the scattering parameters of the material.

Scattering parameters, also known as S-parameters, are a set of complex numbers that describe the behavior of a linear electrical network or device in terms of signal transmission and reflection. They quantify how an electrical signal is transmitted or reflected at various ports of a device. In a two-port network, the S-parameters are typically represented as S11, S12, S21, and S22. S11 represents the reflection coefficient at Port 1, S22 represents the reflection coefficient at Port 2, S12 represents the forward transmission coefficient from Port 1 to Port 2, and S21 represents the reverse transmission coefficient from Port 2 to Port 1.

Before the measurement process, the device is calibrated, and then the measurement quality of the device is tested with air and Teflon. After the permittivity (real part) value of ~1 for air and ~2.1 for Teflon was observed, the measurements of the samples were carried out.

3. Results and Discussion

3.1. Dielectric Properties

Dielectric properties of materials refer to their interaction with electric fields and their electrical conductivity. These properties determine the electrical insulating abilities, energy storage capacities, and other electromagnetic interactions of materials. When an electric field is applied, the charges in the material move or displace, creating a dipole moment. These dipole moments determine the permittivity of the material.

The real permittivity and imaginary permittivity values fully describe the dielectric properties of a material. The real part of permittivity characterizes a material's ability to store energy when exposed to an electric field [11]. Materials with high real permittivity show greater resistance to the electric field and may have higher energy storage capacity [35]. The imaginary permittivity is a measure of the dissipated energy within materials and is primarily related to conductivity [36]. Materials with high imaginary permittivity can cause greater energy loss in the electric field.

The study discovered that the ε' and ε'' of the samples increased across the entire frequency range used as the amount of carbon black in the composition increased. This results in interfacial polarization due to charge accumulation at the interface, so it contributes to the increase of ε' and ε''. For carbon black-filled samples, ε' values from 2.5 to 10 and ε'' values from 0.2 to 4. On the other hand, permittivity values of the graphite-filled samples are very close to each other, as shown in Figure 3. ε' values are in the range 2.5–3 in Figure 3a,b, while ε'' values are 0.1–0.2 in Figure 3c,d. The dielectric parameters of the samples, particularly those containing a relatively higher amount of carbon black, show a frequency-dependent behavior. This is because the movement of electrons under the electric field varies depending on the frequency [37]. The increment in permittivity with the addition of carbon black can be attributed to the formation of more conductive pathways within the sample, as evidenced by the frequency-dependent behavior of the imaginary part of the permittivity.

For carbon black filled samples AC conductivity increases by the increasing amount of filler material, as expected. Conductive filler addition usually enhances electrical conductivity. These values are close to each other in graphite-filled samples, related to the imaginary permittivity values. At high frequencies, almost all the samples showed higher AC conductivity. It appears that the AC conductivity values increase almost linearly as the frequency increases for a single sample composition. The conductivity of a material is primarily controlled by the random diffusion of charge carriers through activated hopping at low frequencies. This results in a conductivity that remains constant regardless of the frequency. However, as the frequency increases, the AC conductivity demonstrates dispersion. It follows a power law relationship, gradually approaching linearity at higher frequencies [39]. The increased frequency can enhance the hopping ability of electrons, leading to their improved capability to move. In the high-frequency region, electrons tend to be highly stimulated and readily move or jump from one particle to another. These particles are either in contact or located near each other [25].

Carbon black-filled samples let a higher AC conductivity than graphite-filled samples. AC conductivity is directly proportional to frequency for all cases in the 1–14 GHz range.

3.2. Shielding Efficiency

For the calculation of the total shielding efficiency (SE_T) in Equation (2), real and imaginary permittivity values are determined. The SE_T can be expressed as the logarithmic ratio of transmitted and incident wave powers. SE_T also can be determined as the sum of the contributions from the three primary shielding mechanisms, which are reflection (SE_R) in Equation (3), absorption (SE_A) in Equation (4), and multiple reflections (SE_{MR}). The significance of SE_{MR} in relation to SE_T is relatively minor compared to SE_A and SE_R. If $SE_T \geq 10$ dB, SE_{MR} is generally considered insignificant. The reflection shielding efficiency (SE_R) is contingent upon the impedance of the medium through which the wave is propagating η_0 denotes the impedance of the medium through which the wave

is propagating. η_s represents the surface impedance. σ is the electrical conductivity. μ' and μ'' are permeability values. t is the thickness in m. Since neither the fillers nor the polymer materials used in the study exhibited any magnetic properties, permeability was not taken into account [25,40]. For the calculation of absorption shielding, it was assumed that the thickness is 2 mm, as stated in the sample preparation title. According to Equation (3), thickness does not affect reflection shielding. Considering Equations (3) and (4), it is expected that the total shielding efficiency will increase as the AC conductivity increases. Additionally, as the frequency increases, the reflection tends to decrease, and the absorption tends to increase.
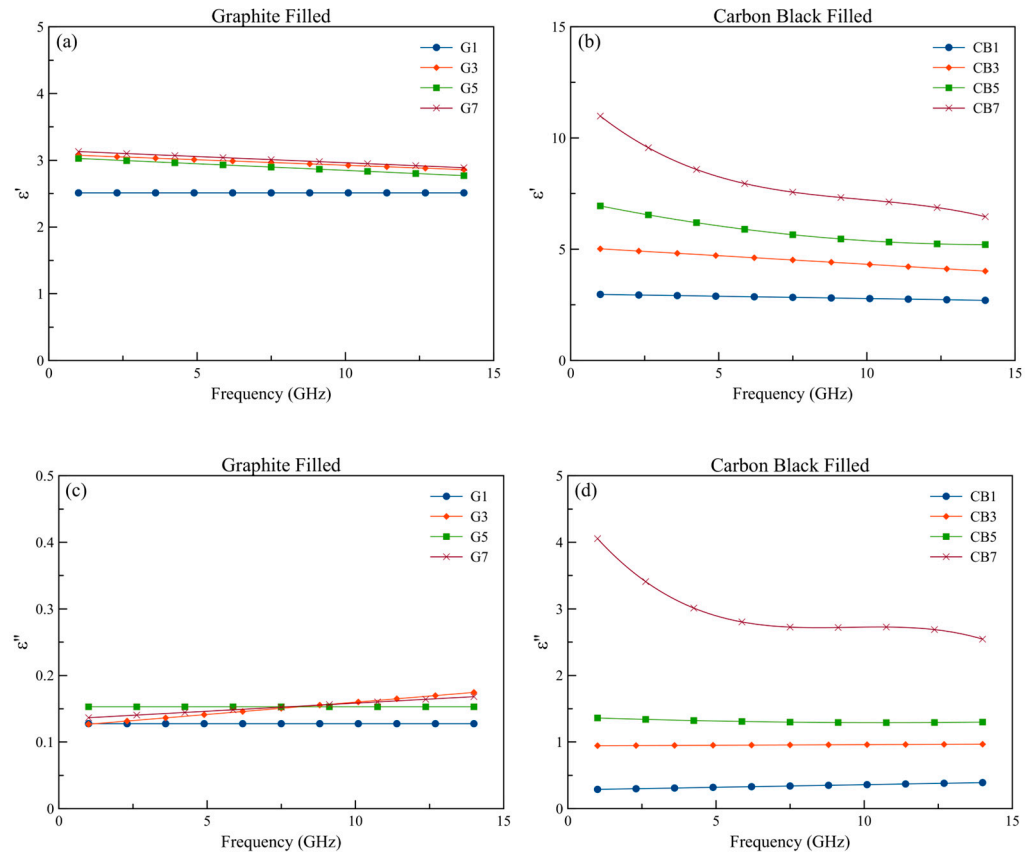

Figure 3. Real (**a**,**b**) and imaginary (**c**,**d**) permittivity values depend on frequency and graphite/carbon black content.

The AC conductivity is calculated with Equation (1). ε_0 is the permittivity of free space (8.854×10^{-12} Fm^{-1}) [38], and f is the frequency in Hertz. ε'' is the imaginary permittivity which is measured by VNA. Frequency-dependent AC conductivity of the presented compositions is illustrated in Figure 4.

$$\sigma_{AC} = 2\pi f \varepsilon_0 \varepsilon'' \tag{1}$$

$$SE_T = 10\log \frac{P_{in}}{P_{out}} = SE_A + SE_R + SE_{MR} \tag{2}$$

$$SE_R(dB) = -20\log \frac{\eta_0}{4\eta_s} = 39.5 + \frac{10\log \sigma}{2\pi f \mu} \tag{3}$$

$$SE_A(dB) = 8.7t\sqrt{\pi \sigma f \mu'} \tag{4}$$
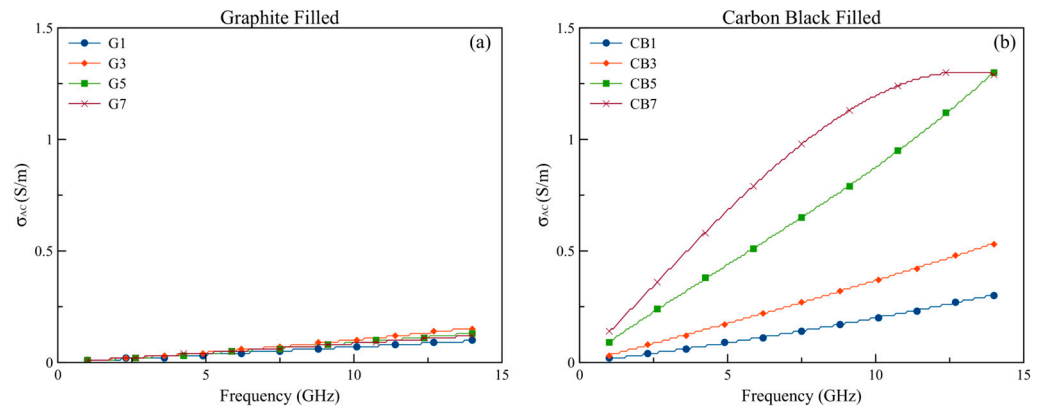
Figure 4. Dependence of AC conductivity values of graphite (**a**) and carbon black (**b**) filled samples on the frequency and compositional parameters.

All samples were assumed to have negligible multiple reflection contributions, and this was not taken into account in the analysis. The decision to ignore multiple reflection contributions was based on the assumption that any re-reflected waves would be absorbed within the material, as the thickness of the material was greater than the critical thickness value known as the skin depth [41].

By increasing the amount of filler, both SE_A and SE_R values tend to increase significantly in the high-frequency region illustrated in Figures 5 and 6. This could be due to the creation of multiple conduction pathways within the bulk structure of the samples. SE_R values are quite high when compared to SE_A for all cases. Both graphite and carbon black filled samples show a lower absorption shielding effectiveness, for graphite filled in the range 0–1.5 dB in Figure 5a and for carbon black filled in the range 0–5 dB in Figure 5b. It is seen in Figure 6 reflection is the main mechanism of the shielding efficiency, which constitutes the majority of total efficiency for all types of samples. Reflection shielding efficiencies are in the range of 19–21 dB for graphite filled in Figure 6a and 8–17 dB for carbon black filled in Figure 6b.
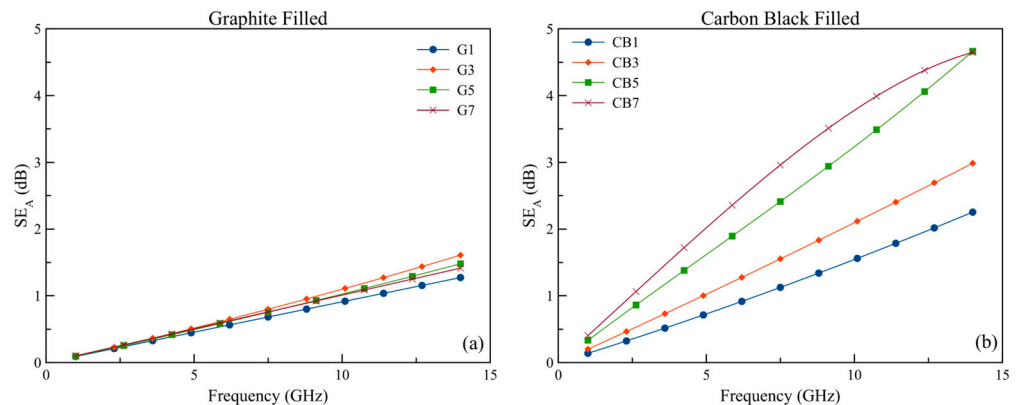

Figure 5. Absorption shielding efficiency values of graphite (**a**) and carbon black (**b**) samples.

Considering graphite samples, SE_R remains almost unchanged in spite of the increasing frequency. On the contrary, SE_A shows an upward movement directly proportional to the frequency of the incident photon. Thus, SE_A and SE_R contributions are important and must be improved at both low and high-frequency regions to develop effective electromagnetic shielding materials.
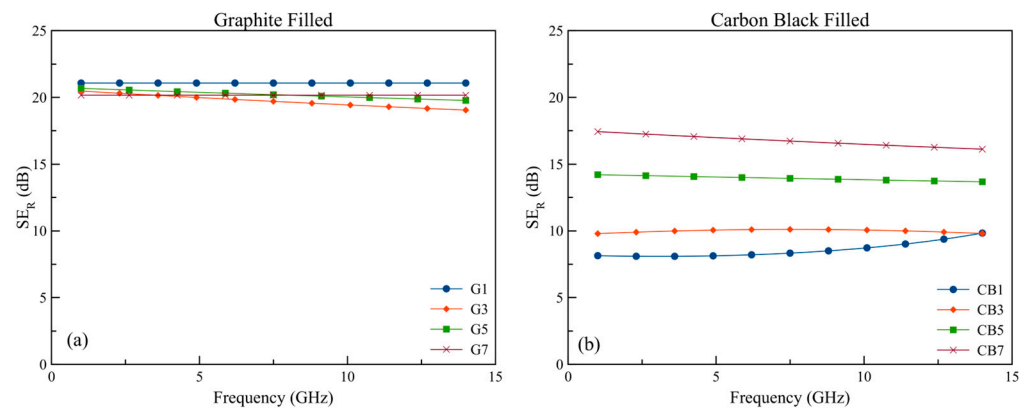
Figure 6. Reflection shielding efficiency values of graphite (**a**) and carbon black (**b**) samples.

The total shielding efficiency of the graphite-added samples is slightly higher than the carbon black-added samples, as shown in Figure 7. SE_T values for graphite-added samples are 20–21 dB for the L band and S band; 19–21 dB for the C band, X band and partially Ku band. As the frequency increases, a small decrease can be mentioned from the L band to the Ku band. For carbon black added samples, it can be said that the SE_T values change little in different band ranges. SE_T for CB1 8 dB in L band, S band and C band; 9 dB in X band and 10 dB in partially Ku band. CB3 is 10 dB, CB5 is 14 dB, and CB7 is 17 dB, and these values remain almost constant from the L band to the Ku band. Although the AC conductivity values of the carbon black-filled samples are higher, the higher shielding efficiency of the graphite-filled samples is due to the segregation of carbon black in the matrix. These values are very close to each other in graphite-added samples, but differences can be observed in carbon black-added samples according to the filling ratio. Graphite's layered structure can lead to higher contact resistance between filler particles, especially at low wt%, hindering the formation of an effective conductive network [42]. This makes graphite composites less sensitive to lower wt% filler content for achieving good EMI shielding performance. When working with higher graphite filler ratios, it is predicted that these SE_T values will not be close to each other. Shielding efficiency values change as the carbon black filler ratio increases. Generally, it can be said that the results in this study show consistency when compared to other studies shown in Table 3. It's important to consider that the provided Table 3 includes different filler amounts, concentration levels, production methods and frequency ranges for various materials and composites. The specific performance may vary based on factors such as the dispersion of the filler and the measurement setup.
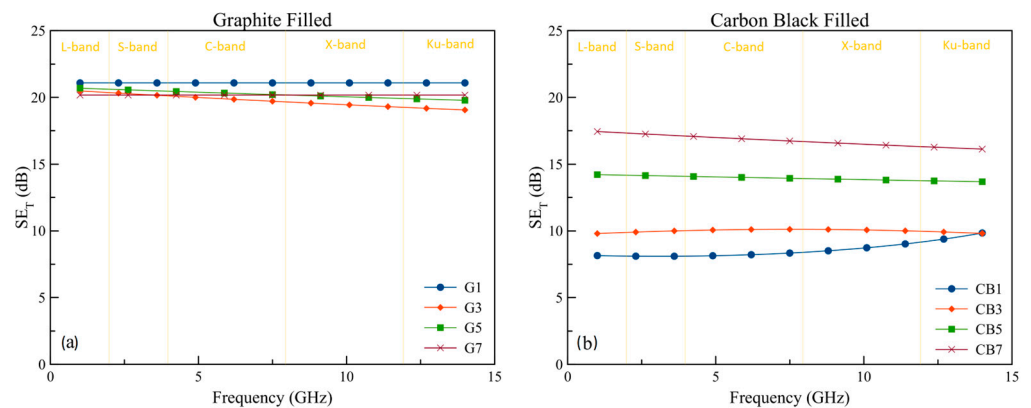

Figure 7. Total shielding efficiency values of graphite (**a**) and carbon black (**b**) samples.

Table 3. EMI SE values of different polymer matrix composites were reported in earlier studies.

Matrix	Filler	Filler Amount wt. %	EMI SE (dB)	Frequency Range (GHz)	Ref.
Polyurethane	CB	6.51	13–14	8–18	[43]
Ethylene Methyl Acrylate	CB	10	10	8.2–12.4	[44]
Epoxy	CB	30	44	1–10	[45]
Polypropylene	CB	22.5	17–20	5.5–8	[46]
Polyurethane	Graphite	20	20	8.2–12.3	[47]
Polyaniline	Graphite	20	18–5	2.5–2.7	[48]
Polypropylene	Graphite	20	10.3	8–12	[49]
Polypropylene	Graphite Carbon fiber	20	44.43	8–12	[50]

The shielding efficiencies of the samples with both types of filling materials vary little depending on the frequency. This is important in terms of keeping the efficiency of the shielding material constant in applications in the 1–14 GHz range.

4. Conclusions

The aim of this study is to examine the dielectric properties of epoxy composites filled with graphite and carbon black for potential use as electromagnetic interference (EMI) shielding material. Composite materials are produced by mechanical mixing. Samples have different filling ratios between 1 and 7 wt%. The coaxial method is used to obtain these properties in the frequency range of 1–14 GHz at the Vector Network Analyzer. The results showed that the addition of fillers significantly affected the dielectric and shielding properties of the composites. The real part of permittivity (ε') increased with increasing amounts of carbon black in the composition, while the permittivity values of graphite-filled samples were very close to each other. On the other hand, the imaginary part of permittivity (ε'') increased across the entire frequency range used as the amount of carbon black increased. This frequency-dependent behavior of ε'' suggests the formation of more conductive pathways within the sample.

Measurements show that although carbon black-filled samples have more AC conductivity, graphite-filled samples' shielding efficiencies are higher. The graphite-added samples exhibited a slightly higher SE_T of 19–21 dB compared to the carbon black-added samples, which had a SE_T of 8–17 dB. The epoxy composites with graphite filler tend to exhibit higher shielding efficiency compared to the epoxy composites with carbon black filler due to the segregation of carbon black. In the graphite-added samples, different filling ratios resulted in a more consistent shielding behavior compared to the carbon black-added coatings. However, increasing the carbon-black filler ratio resulted in higher shielding efficiency. The shielding efficiencies of both types of filling materials showed little variation with frequency. Overall, the results suggest that composite materials containing carbon black and graphite fillers look promising and have a good potential for isolating static structures. After the epoxy matrix composite shielding material is produced and cured in plate-shaped molds, it can be used by sticking to the walls of the structure to be shielded with a suitable adhesive.

Graphite-filled shielding materials have higher shielding efficiency at lower rates than carbon black, and it can be advantageous for low-cost applications. Carbon black-added shielding materials can be more effective if they are used with higher than 7 wt% filling ratios. Since carbon black has fine particle size, sample integrity could not be achieved in compositions above 7 wt% in the mechanical mixing method. For this, it may be necessary to adopt a different production method, but this may be a factor that increases the production cost.

References

1. Song, Y.L.; Reddy, M.K.; Wen, H.Y.; Chang, L.M. Mitigation of Electro Magnetic Interference by Using C-Shaped Composite Cylindrical Device. *Appl. Sci.* **2022**, *12*, 882. [CrossRef]
2. Liang, C.; Qiu, H.; Song, P.; Shi, X.; Kong, J.; Gu, J. Ultra-light MXene aerogel/wood-derived porous carbon composites with wall-like 'mortar/brick' structures for electromagnetic interference shielding. *Sci. Bull.* **2020**, *65*, 616–622. [CrossRef]
3. Bhargav, H.; Srinivasan, T.M.; Varambally, S.; Gangadhar, B.N.; Koka, P.S. Effect of mobile phone-induced electromagnetic field on brain hemodynamics and human stem cell functioning: Possible mechanistic link to cancer risk and early diagnostic value of electronphotonic imaging. *Stem Cells Mediat. Regen.* **2016**, *10*, 263–274.
4. Kabuto, M.; Nitta, H.; Yamamoto, S.; Yamaguchi, N.; Akiba, S.; Honda, Y.; Hagihara, J.; Isaka, K.; Saito, T.; Ojima, T.; et al. Childhood leukemia and magnetic fields in Japan: A case-control study of childhood leukemia and residential power-frequency magnetic fields in Japan. *Int. J. Cancer* **2006**, *119*, 643–650. [CrossRef] [PubMed]
5. Martel, J.; Chang, S.H.; Chevalier, G.; Ojcius, D.M.; Young, J.D. Influence of electromagnetic fields on the circadian rhythm: Implications for human health and disease. *Biomed. J.* **2023**, *46*, 48–59. [CrossRef]
6. Lim, H.; Choi, J.; Joo, H.; Ha, M. Exposures to radio-frequency electromagnetic fields and their impacts on children's health—What the science knows? *Curr. Opin. Environ. Sci. Health* **2023**, *32*, 100456. [CrossRef]
7. Database of Frequency Allocations. Available online: http://www.classic.grss-ieee.org/frequency_allocations.html (accessed on 22 July 2023).
8. Geetha, S.; Kumar, K.K.S.; Rao, C.R.K.; Vijayan, M.; Trivedi, D.C. EMI shielding: Methods and materials—A review. *J. Appl. Polym. Sci.* **2009**, *112*, 2073–2086. [CrossRef]
9. Elmahaishi, M.F.; Azis, R.S.; Ismail, I.; Muhammad, F.D. A review on electromagnetic microwave absorption properties: Their materials and performance. *J. Mater. Res. Technol.* **2022**, *20*, 2188–2220. [CrossRef]
10. Fan, Y.; Yang, H.; Li, M.; Zou, G. Evaluation of the microwave absorption property of flake graphite. *Mater. Chem. Phys.* **2009**, *115*, 696–698. [CrossRef]
11. Wang, X.-X.; Zheng, Q.; Zheng, Y.-J.; Cao, M.-S. Green EMI shielding: Dielectric/magnetic 'genes' and design philosophy. *Carbon* **2023**, *206*, 124–141. [CrossRef]
12. Krishnasamy, J.; Thilagavathi, G.; Alagirusamy, R.; Das, A. Metal-embedded matrices for EMI shielding. In *Materials for Potential EMI Shielding Applications*; Elsevier: Amsterdam, The Netherlands, 2020; pp. 111–120. [CrossRef]
13. Chen, X.; Gu, Y.; Liang, J.; Bai, M.; Wang, S.; Li, M.; Zhang, Z. Enhanced microwave shielding effectiveness and suppressed reflection of chopped carbon fiber felt by electrostatic flocking of carbon fiber. *Compos. Part A Appl. Sci. Manuf.* **2020**, *139*, 106099. [CrossRef]
14. Ma, T.; Yan, M.; Wang, W. The evolution of microstructure and magnetic properties of Fe-Si-Al powders prepared through melt-spinning. *Scr. Mater.* **2008**, *58*, 243–246. [CrossRef]
15. Chithra, A.; Wilson, P.; Vijayan, S.; Rajeev, R.; Prabhakaran, K. Thermally insulating robust carbon composite foams with high EMI shielding from natural cotton. *J. Mater. Sci. Technol.* **2021**, *94*, 113–122. [CrossRef]
16. Chiba, S.; Waki, M. Verification of the radio wave absorption effect in the millimeter wave band of swcnts and conventional carbon-based materials. *Appl. Sci.* **2021**, *11*, 11490. [CrossRef]
17. Abbasi, H.; Antunes, M.; Velasco, J.I. Recent advances in carbon-based polymer nanocomposites for electromagnetic interference shielding. *Prog. Mater. Sci.* **2019**, *103*, 319–373. [CrossRef]
18. Kamkar, M.; Ghaffarkhah, A.; Hosseini, E.; Amini, M.; Ghaderi, S.; Arjmand, M. Multilayer polymeric nanocomposites for electromagnetic interference shielding: Fabrication, mechanisms, and prospects. *New J. Chem.* **2021**, *45*, 21488–21507. [CrossRef]
19. Amini, M.; Kamkar, M.; Rahmani, F.; Ghaffarkhah, A.; Ahmadijokani, F.; Arjmand, M. Multilayer Structures of a $Zn_{0.5}Ni_{0.5}Fe_2O_4$-Reduced Graphene Oxide/PVDF Nanocomposite for Tunable and Highly Efficient Microwave Absorbers. *ACS Appl. Electron. Mater.* **2021**, *3*, 5514–5527. [CrossRef]

20. Zhou, M.; Gu, W.; Wang, G.; Zheng, J.; Pei, C.; Fan, F.; Ji, G. Sustainable wood-based composites for microwave absorption and electromagnetic interference shielding. *J. Mater. Chem A Mater.* **2020**, *8*, 24267–24283. [CrossRef]

21. Wei, Y.; Liang, D.; Zhou, H.; Huang, S.; Zhang, W.; Gu, J.; Hu, C.; Lin, X. Facile preparation of MXene-decorated wood with excellent electromagnetic interference shielding performance. *Compos. Part A Appl. Sci. Manuf.* **2022**, *153*, 106739. [CrossRef]

22. Stupar, S.L.; Vuksanović, M.M.; Mijin, D.; Milanović, B.C.; Joksimović, V.J.; Barudžija, T.S.; Knežević, M.R. Multispectral electromagnetic shielding and mechanical properties of carbon fabrics reinforced by silver deposition. *Mater. Chem. Phys.* **2022**, *289*, 126495. [CrossRef]

23. Ryu, S.H.; Han, Y.K.; Kwon, S.J.; Kim, T.; Jung, B.M.; Lee, S.-B.; Park, B. Absorption-dominant, low reflection EMI shielding materials with integrated metal mesh/TPU/CIP composite. *Chem. Eng. J.* **2022**, *428*, 131167. [CrossRef]

24. Drakakis, E.; Kymakis, E.; Tzagkarakis, G.; Louloudakis, D.; Katharakis, M.; Kenanakis, G.; Suchea, M.; Tudose, V.; Koudoumas, E. A study of the electromagnetic shielding mechanisms in the GHz frequency range of graphene based composite layers. *Appl. Surf. Sci.* **2017**, *398*, 15–18. [CrossRef]

25. Kasgoz, A.; Korkmaz, M.; Alanalp, M.B.; Durmus, A. Effect of processing method on microstructure, electrical conductivity and electromagnetic wave interference (EMI) shielding performance of carbon nanofiber filled thermoplastic polyurethane composites. *J. Polym. Res.* **2017**, *24*, 148. [CrossRef]

26. Yalcin, G.E.; Esen, H.E.; Yagimli, M.; Arca, E. Mathematical modelling of sound transmission loss (STL) in metallic and graphite based coatings. *Trans. Inst. Met. Finish.* **2022**, *100*, 85–92. [CrossRef]

27. Zahedi, S.; Ghaffarian, S.R. A new approach to design of anti-corrosive three layers self-stratifying coatings. *Trans. Inst. Met. Finish.* **2021**, *99*, 133–140. [CrossRef]

28. Chung, D.D.L. Electromagnetic interference shielding effectiveness of carbon materials. *Carbon* **2001**, *39*, 279–285. [CrossRef]

29. Tian, K.; Hu, D.; Wei, Q.; Fu, Q.; Deng, H. Recent progress on multifunctional electromagnetic interference shielding polymer composites. *J. Mater. Sci. Technol.* **2023**, *134*, 106–131. [CrossRef]

30. Mohapatra, P.P.; Ghosh, S.; Jain, A.; Aich, S.; Dobbidi, P. Rare earth substituted lithium ferrite/carbon black ceramic composites for shielding electromagnetic radiation. *J. Magn. Magn. Mater.* **2023**, *573*, 170678. [CrossRef]

31. Yadav, A.; Tripathi, K.C.; Baskey, H.B.; Alegaonkar, P.S. Microwave scattering behaviour of carbon black/ molybdenum di sulphide /cobalt composite for electromagnetic interference shielding application. *Mater. Chem. Phys.* **2022**, *279*, 125766. [CrossRef]

32. Yan, C.; Shi, Y.; Li, Z.; Wen, S.; Wei, Q. Research on preparation and forming technologies of selective laser sintering polymer materials. In *Selective Laser Sintering Additive Manufacturing Technology*; Academic Press: Cambridge, MA, USA, 2021; pp. 251–500. [CrossRef]

33. Bartley, P.G.; Begley, S.B. A new technique for the determination of the complex permittivity and permeability of materials. In Proceedings of the 2010 IEEE International Instrumentation and Measurement Technology Conference, I2MTC 2010, Austin, TX, USA, 3–6 May 2010; pp. 54–57. [CrossRef]

34. Rothwell, E.J.; Frasch, J.L.; Ellison, S.M.; Chahal, P.; Ouedraogo, R.O. Analysis of the Nicolson-Ross-Weir Method for Characterizing the Electromagnetic Properties of Engineered Materials. *Prog. Electromagn. Res.* **2016**, *157*, 31–47. [CrossRef]

35. Kar, S. *High Permittivity Gate Dielectric Materials*; Springer Series in Advanced Microelectronics; Springer: Berlin/Heidelberg, Germany, 2013; Volume 43. [CrossRef]

36. Tataroğlu, A. Dielectric permittivity, ac conductivity and electric modulus properties of metal/ferroelectric/semiconductor (MFS) structures. *Gazi Univ. J. Sci.* **2013**, *26*, 501–508.

37. Sadiku, M.N.O. *Elements of Electromagnetics*, 7th ed.; Oxford University Press: New York, NY, USA, 2018.

38. Shivaraja, S.J.; Mishra, S.; Dutta, K.; Gupta, R.K.; Manjuladevi, V. Frequency dependence of dielectric permittivity and conductivity of functionalized carbon nanotube-nematic liquid crystal nanocomposite. *J. Mol. Liq.* **2022**, *349*, 118168. [CrossRef]

39. Tsonos, C. Comments on frequency dependent AC conductivity in polymeric materials at low frequency regime. *Curr. Appl. Phys.* **2019**, *19*, 491–497. [CrossRef]

40. Kasgoz, A.; Korkmaz, M.; Durmus, A. Compositional and structural design of thermoplastic polyurethane/carbon based single and multi-layer composite sheets for high-performance X-band microwave absorbing applications. *Polymer* **2019**, *180*, 121672. [CrossRef]

41. Al-Saleh, M.H.; Sundararaj, U. Electromagnetic interference shielding mechanisms of CNT/polymer composites. *Carbon* **2009**, *47*, 1738–1746. [CrossRef]

42. Zeodinov, M.G.; Kostanovskiy, A.V.; Kostanovskaya, M.E.; Pronkin, A.A. Electrical Contact Resistance of Graphite. *High Temp.* **2022**, *60*, 469–473. [CrossRef]

43. Gupta, K.K.; Abbas, S.M.; Abhyankar, A.C. Carbon black/polyurethane nanocomposite-coated fabric for microwave attenuation in X & Ku-band (8–18 GHz) frequency range. *J. Ind. Text.* **2016**, *46*, 510–529. [CrossRef]

44. Mondal, S.; Ganguly, S.; Das, P.; Khastgir, D.; Das, N.C. Low percolation threshold and electromagnetic shielding effectiveness of nano-structured carbon based ethylene methyl acrylate nanocomposites. *Compos. B Eng.* **2017**, *119*, 41–56. [CrossRef]

45. Aal, N.A.; El-Tantawy, F.; Al-Hajry, A.; Bououdina, M. New antistatic charge and electromagnetic shielding effectiveness from conductive epoxy resin/plasticized carbon black composites. *Polym. Compos.* **2008**, *29*, 125–132. [CrossRef]

46. Wu, M.; Wu, F.; Ren, Q.; Jia, X.; Luo, H.; Shen, B.; Wang, L.; Zheng, W. Tunable electromagnetic interference shielding performance of polypropylene/carbon black composites via introducing microcellular structure. *Compos. Commun.* **2022**, *36*, 101363. [CrossRef]

47.   Valentini, M.; Piana, F.; Pionteck, J.; Lamastra, F.R.; Nanni, F. Electromagnetic properties and performance of exfoliated graphite (EG)—Thermoplastic polyurethane (TPU) nanocomposites at microwaves. *Compos. Sci. Technol.* **2015**, *114*, 26–33. [CrossRef]

48.   Mathew, K.T.; Kalappura, U.G.; Augustine, R.; Jean-Marc, L.; Lakshmi, K. Enhanced EMI shielding efficiency using carbon, graphite, and polyaniline blends. *Microw. Opt. Technol. Lett.* **2010**, *52*, 393–397. [CrossRef]

49.   Kaushal, A.; Singh, V. Melt-Processed Graphite-Polypropylene Composites for EMI Shielding Applications. *J. Electron. Mater.* **2020**, *49*, 5293–5301. [CrossRef]

50.   Kaushal, A.; Singh, V. Analysis of mechanical, thermal, electrical and EMI shielding properties of graphite/carbon fiber reinforced polypropylene composites prepared via a twin screw extruder. *J. Appl. Polym. Sci.* **2022**, *139*, 51444. [CrossRef]